Inorg. Chem. **2008**, *47*, 2849−2857

A [4Fe−4S] Cluster Dimer Bridged by Bis(2,2′:6′,2″-terpyridine-4′-thiolato)iron(II)

Erwin P. L. van der Geer,[†] Gerard van Koten,[†] Robertus J. M. Klein Gebbink,*[,†] and Bart Hessen*[,†,‡]

Chemical Biology & Organic Chemistry, Faculty of Science, Utrecht University, Padualaan 8, 3584 CH Utrecht, The Netherlands, and Stratingh Institute, University of Groningen, Nijenborgh 4, 9747 AG Groningen, The Netherlands

Received October 18, 2007

The use of 2,2′:6′,2″-terpyridine-4′-thiol (tpySH) was explored as a bridging ligand for the formation of stable assemblies containing both [4Fe−4S] clusters and single metal ions. Reaction of tpySH (2 equiv) with $(NH_4)_2Fe(SO_4)_2 \cdot 6H_2O$ generated the homoleptic complex $[Fe(tpySH)_2]^{2+}$, which was isolated as its PF_6^- salt. The compound could be fully deprotonated to yield neutral $[Fe(tpyS)_2]$, and the absorption spectrum is highly dependent on the protonation state. Reaction of $[Fe(tpySH)_2](PF_6)_2$ with the new 3:1 site-differentiated cluster (n-$Bu_4N)_2[Fe_4S_4(TriS)(SEt)]$ yielded the first metal-bridged [4Fe−4S] cluster dimer, $(n\text{-}Bu_4N)_2[\{Fe_4S_4(TriS)(\mu\text{-}Stpy)\}_2Fe]$. Electrochemical studies indicate that the [4Fe−4S] clusters in the dimer act as independent redox units, while UV–vis spectroscopy provides strong evidence for a thioquinonoid electron distribution in the bridging $tpyS^-$ ligand. TpySH thus acts as a directional bridging ligand between [4Fe−4S] clusters and single metal ions, thereby opening the way to the synthesis of larger, more complex assemblies.

Introduction

Cubane-type [4Fe−4S] clusters play important roles in many proteins, including electron transport, sensing, and structural stabilization.[1,2] In some enzymes, a [4Fe−4S] cluster forms an integral part of the active site, with the cluster being either catalytically active itself or linked via bridging cysteine residues to a catalytic mono- or dimetallic subsite. For example, in the H cluster of Fe-only hydrogenase, a [4Fe−4S] cluster is bound via a bridging cysteine residue to a [2Fe−2S] subsite where the actual catalysis is believed to take place.[3] Similarly, [4Fe−4S] clusters in the active sites of acetyl coenzyme A synthase/carbon monoxide dehydrogenase[4] and sulfite reductase[5] are bridged to a [2Ni−2S] subsite and a siroheme group, respectively.

Intrigued by the influence of the [4Fe−4S] cluster on the bridged, metal-containing subsite, several researchers have incorporated [4Fe−4S] clusters into active-site models. Holm and co-workers mimicked the sulfite reductase active site by binding a [4Fe−4S] cluster to siroheme analogues via bridging sulfide ions.[6] Pickett and co-workers employed the same cluster in their synthesis of a thiolate-bridged model of the Fe-only hydrogenase H cluster.[7] Meanwhile, Pohl and co-workers reported the synthesis of assemblies of nickel(II) thiolates and [4Fe−4S] clusters in the context of mimicking the carbon monoxide dehydrogenase active site.[8]

In all of these biomimetic studies, the bridging ligands were chosen to reflect most closely the modeled active-site architectures. However, a selective and more general bridging ligand would allow for a systematic method of forming stable complexes of [4Fe−4S] clusters and other metals. This not only would be of interest in the synthesis of new biomimetic systems but also would facilitate potential future applications

* To whom correspondence should be addressed. E-mail: r.j.m.kleingebbink@uu.nl (R.J.M.K.G.), b.hessen@rug.nl (B.H.).
† Utrecht University.
‡ University of Groningen.

(1) Beinert, H.; Holm, R. H.; Münck, E. *Science* **1997**, *277*, 653–659.
(2) Johnson, M. K. *Curr. Opin. Chem. Biol.* **1998**, *2*, 173–181.
(3) (a) Nicolet, Y.; Piras, C.; Legrand, P.; Hatchikian, C. E.; Fontecilla-Camps, J. C. *Structure* **1999**, *7*, 13–23. (b) Peters, J. W.; Lanzilotta, W. N.; Lemon, B. J.; Seefeldt, L. C. *Science* **1998**, *282*, 1853–1858.
(4) (a) Doukov, T. I.; Iverson, T. M.; Seravalli, J.; Ragsdale, S. W.; Drennan, C. L. *Science* **2002**, *298*, 567–572. (b) Darnault, C.; Volbeda, A.; Kim, E. J.; Legrand, P.; Vernede, Z.; Lindahl, P. A.; Fontecilla-Camps, J. C. *Nat. Struct. Biol.* **2003**, *10*, 271–279.
(5) Crane, B. R.; Siegel, L. M.; Getzoff, E. D. *Science* **1995**, *270*, 59–67.
(6) (a) Cai, L.; Weigel, J. A.; Holm, R. H. *J. Am. Chem. Soc.* **1993**, *115*, 9289–9290. (b) Cai, L.; Holm, R. H. *J. Am. Chem. Soc.* **1994**, *116*, 7177–7188. (c) Zhou, C.; Cai, L.; Holm, R. H. *Inorg. Chem.* **1996**, *35*, 2767–2772.
(7) Tard, C.; Liu, X.; Ibrahim, S. K.; Bruschi, M.; De Gioia, L.; Davies, S. C.; Yang, X.; Wang, L.-S.; Sawers, G.; Pickett, C. J. *Nature* **2005**, *433*, 610–613.
(8) (a) Osterloh, F.; Saak, W.; Pohl, S. *J. Am. Chem. Soc.* **1997**, *119*, 5648–5656. (b) Osterloh, F.; Saak, W.; Haase, D.; Pohl, S. *Chem. Commun.* **1996**, 777–778.

10.1021/ic702062q CCC: $40.75
Published on Web 03/11/2008

Scheme 1. Thiol and Thione Tautomers of tpySH

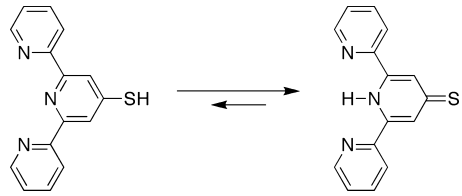

of [4Fe−4S] clusters as conducting or redox-active units in smart materials such as nanoelectronic devices.[9] Ideally, such a general ligand would contain two distinct metal-binding groups: one group that has a preference for strong binding to single metal ions and one thiol group for binding to [4Fe−4S] clusters.

A ligand that attractively fulfills these requirements is 2,2′:6′,2″-terpyridine-4′-thiol (tpySH), first reported by McEuen, Ralph, and co-workers in 2002.[10] The ligand was shown to bind Co^{2+} ions as an N,N,N-tridentate chelate, thereby leaving the thiol group available for binding to Au surfaces. Three years later, Constable and co-workers reported a more convenient synthesis of tpySH and demonstrated that, both in solution and in the solid state, the thione tautomer of tpySH is favored over the thiol (Scheme 1).[11] Furthermore, the authors showed that, after oxidation to the corresponding disulfide, tpySH can coordinate to Fe^{2+} ions to form metallomacrocyclic compounds. Inspired by these reports, we decided to attempt the use of tpySH as a bridge between Fe^{2+} ions and [4Fe−4S] clusters.

Experimental Section

General Procedures. All air-sensitive compounds were handled in a glovebox or using standard Schlenk techniques. $AgNO_3$ (Acros), NaH (Acros, 60% dispersion in mineral oil), $(NH_4)_2Fe(SO_4)_2 \cdot 6H_2O$ (Aldrich), and NH_4PF_6 (Acros) were used as received. Triethylamine (Acros) and chloromethyl ethyl ether (Aldrich) were degassed prior to use. Tetrahydrofuran (THF) and diethyl ether were distilled from Na/benzophenone, CH_2Cl_2 and dimethylformamide (DMF) were distilled from CaH_2, and pentane was distilled from Na. MeCN was distilled from $KMnO_4$ and Na_2CO_3 prior to use in cyclic voltammetry.[12] Solvents for air-sensitive compounds were thoroughly degassed or flushed with N_2. ^1H and ^{13}C NMR spectra were recorded at 298 K on a Varian 400 MHz spectrometer operating at 400 and 100 MHz, respectively, or at 300 K on a Bruker AC 300 spectrometer operating at 300 and 75 MHz, respectively. Spectra were calibrated on the residual solvent peaks. Signal assignments were based on chemical shift, integral, and line-width considerations, as well as 2D COSY ^1H NMR for **6** and **7**. IR spectra were recorded on a Perkin-Elmer Spectrum One FT-IR spectrometer. UV–vis spectra were recorded on a Varian Cary 50 Scan UV–visible spectrophotometer. The electrospray ionization (ESI) mass spectrum of **5** was recorded on an API 3+ triple-quadrupole mass spectrometer (Sciex, Concord, Ontario, Canada) equipped with a modified pneumatically assisted electrospray (IonSpray) interface.[13] The homemade front cover and the IonSpray interface ensure a gastight ion source. The atmospheric pressure ion source was first evacuated and then filled with dry N_2. N_2 was used as nebulizing and curtain gases. Sample preparation took place in a N_2-filled glovebox. The syringe pump used for sample introduction was also placed inside the glovebox, and a 1.6-mm-o.d., 0.3-mm-i.d. Teflon tube was connected between the syringe pump and the IonSpray interface. Mass spectra were recorded in negative ion mode as Q1 scans with a step size of 0.1 and a dwell time of 1 ms. The electrospray probe capillary voltage was set at 4.0 kV and the cone voltage at 35 V. The ESI mass spectrum of **6** was recorded on a Micromass LC-TOF mass spectrometer by the Biomolecular Mass Spectrometry group at Utrecht University. Elemental analyses were carried out by Kolbe Mikroanalytisches Laboratorium (Mülheim an der Ruhr, Germany). Cyclic voltammograms were recorded at 100 mV/s using Pt working and counter electrodes and a Ag/AgCl reference electrode. The supporting electrolyte was 0.1 M n-Bu_4NClO_4 in CH_2Cl_2 for **5** and **7** and 0.1 M n-Bu_4NPF_6 in MeCN for **6**. Potentials were referenced to a ferrocene (Fc) internal standard. To facilitate comparison with literature values, potentials versus a standard calomel electrode (SCE) were calculated by taking $E_{1/2}$ (Fc/Fc^+) = 0.424 V vs SCE in CH_2Cl_2[14] and 0.379 V in MeCN.[15]

Harris[16] previously reported the syntheses of 3-thiouroniumindole iodide (**1**) and indole-3-thiol (**2**), but did not give full experimental details or spectral characterizations. For convenience, we have included these data as Supporting Information.

3-(Ethoxymethylsulfanyl)indole (3). Thiol **2** (3.95 g, 26.5 mmol) was dissolved in THF (20 mL) and the resulting yellow solution cooled to 0 °C. Triethylamine (3.72 mL, 26.5 mmol) and chloromethyl ethyl ether (2.46 mL, 26.5 mmol) were subsequently added. Within minutes, a white precipitate formed, and the mixture was warmed to ambient temperature and stirred for an extra 24 h. The solution was then poured into water (40 mL) and extracted with ether (3 × 40 mL). The combined organic extracts were washed with an aqueous 1 M HCl solution (1 × 40 mL), water (1 × 40 mL), and brine (1 × 40 mL). The organic phase was dried over $MgSO_4$ and evaporated to yield a yellow oil. Yield: 4.95 g (24.0 mmol, 91%). Anal. Calcd for $C_{11}H_{13}NOS$: C, 63.74; H, 6.32; N, 6.76; S, 15.47. Found: C, 63.59; H, 6.35; N, 6.82; S, 15.38. ^1H NMR (300 MHz, $CDCl_3$): δ 8.27 (s, broad 1 H, NH), 7.79–7.74 (m, 1 H, indolyl H), 7.40–7.36 (m, 1 H, indolyl H), 7.35 (d, $^3J_{H-H}$ = 2.5 Hz, 1 H, indolyl H2), 7.26–7.17 (m, 2 H, indolyl H), 4.77 (s, 2 H, SCH_2O), 3.72 (q, $^3J_{H-H}$ = 7.1 Hz, 2 H, CH_2CH_3), 1.23 (t, $^3J_{H-H}$ = 7.1 Hz, 3 H, CH_2CH_3). $^{13}C\{^1H\}$ NMR (75 MHz, $CDCl_3$): δ 136.26, 129.46, 129.34, 122.71, 120.53, 119.33, 111.59 (7 × indolyl C), 105.11 (indolyl CS), 77.85 (SCH_2O), 64.12 (CH_2CH_3), 15.00 (CH_2CH_3). FT-IR (ATR, ν, cm^{-1}): 3402, 3302, 2974, 2878, 1454, 1407, 1338, 1302, 1260, 1236, 1064, 1008, 944, 833, 740, 675.

1,3,5-Triethyl-2,4,6-tris(3-ethoxymethylsulfanyl)indolyl[1]-methyl)benzene (4). NaH (60% dispersion in mineral oil, 0.960 g, 24.0 mmol) was washed with pentane. A solution of **3** (3.96 g, 19.2 mmol) in THF (100 mL) cooled to 0 °C was then added slowly under constant stirring. After 5 min, the mixture was allowed to warm to ambient temperature and was left stirring overnight. The resulting turbid, orange solution was again cooled to 0 °C, and 1,3,5-

(9) Cao, G. *Nanostructures & Nanomaterials: Synthesis, Properties & Applications*; Imperial College Press: London, U.K., 2004.
(10) Park, J.; Pasupathy, A. N.; Goldsmith, J. I.; Chang, C.; Yaish, Y.; Petta, J. R.; Rinkoski, M.; Sethna, J. P.; Abruña, H. D.; McEuen, P. L.; Ralph, D. C. *Nature* **2002**, *417*, 722–725.
(11) Constable, E. C.; Hermann, B. A.; Housecroft, C. E.; Neuburger, M.; Schaffner, S.; Scherer, L. J. *New J. Chem.* **2005**, *29*, 1475–1481.
(12) Cauquis, G.; Fahmy, H. M.; Pierre, G.; Elnagdi, M. H. *Electrochim. Acta* **1979**, *24*, 391–394.
(13) Bruins, A. P.; Covey, T. R.; Henion, J. D. *Anal. Chem.* **1987**, *59*, 2642–2646.
(14) Masui, M.; Sayo, H.; Tsuda, Y. *J. Chem. Soc. B* **1968**, 973–976.
(15) Kolthoff, I. M.; Thomas, F. G. *J. Phys. Chem.* **1965**, *69*, 3049–3058.
(16) Harris, R. L. N. *Tetrahedron Lett.* **1969**, 4465–4466.

triethyl-2,4,6-tris(bromomethyl)benzene[17] (2.60 g, 5.91 mmol) was added. A white precipitate formed immediately. The mixture was then heated to reflux for 1 h. After cooling to ambient temperature, water (150 mL) was added and the mixture was extracted with ether (3 × 75 mL). The combined organic extracts were washed with water (1 × 75 mL) and brine (1 × 75 mL), dried over $MgSO_4$, and evaporated to yield a pink solid. The product was purified over silica, using EtOAc/hexanes, 30/70 (v/v), as the eluent. Yield: 4.58 g (5.58 mmol, 94%). Anal. Calcd for $C_{48}H_{57}N_3O_3S_3$: C, 70.29; H, 7.00; N, 5.12; S, 11.73. Found: C, 70.22; H, 7.08; N, 4.97; S, 11.77. ^{1}H NMR (300 MHz, acetone-d_6): δ 7.71 (d, $^3J_{H-H}$ = 8.0 Hz, 3 H, indolyl H), 7.66 (d, $^3J_{H-H}$ = 8.3 Hz, 3 H, indolyl H), 7.29 (td, $^3J_{H-H}$ = 7.6 Hz, $^4J_{H-H}$ = 1.2 Hz, 3 H, indolyl H), 7.19 (td, $^3J_{H-H}$ = 7.5 Hz, $^4J_{H-H}$ = 1.0 Hz, 3 H, indolyl H), 6.89 (s, 3 H, indolyl H2), 5.55 (s, 6 H, NCH_2), 4.67 (s, 6 H, SCH_2O), 3.61 (q, $^3J_{H-H}$ = 7.1 Hz, 6 H, OCH_2CH_3), 2.76 (q, $^3J_{H-H}$ = 7.4 Hz, 6 H, aryl CH_2CH_3), 1.03 (t, $^3J_{H-H}$ = 7.1 Hz, 9 H, OCH_2CH_3), 0.96 (t, $^3J_{H-H}$ = 7.6 Hz, 9 H, aryl CH_2CH_3). ^{13}C{^{1}H} NMR (75 MHz, acetone-d_6): δ 147.03 (aryl C), 137.95 (indolyl C), 131.98, 131.84, 131.25 (2 × indolyl C, 1 × aryl C), 123.17, 121.14, 120.27, 110.86 (4 × indolyl C), 104.59 (indolyl CS), 78.44 (SCH_2O), 64.04 (OCH_2CH_3), 44.64 (NCH_2), 24.12 (aryl CH_2CH_3), 15.57 (aryl CH_2CH_3 or OCH_2CH_3), 15.26 (aryl CH_2CH_3 or OCH_2CH_3). FT-IR (ATR, ν, cm^{-1}): 3049, 2970, 2930, 2872, 1610, 1505, 1451, 1391, 1336, 1296, 1219, 1160, 1081, 1011, 838, 738, 668.

1,3,5-Triethyl-2,4,6-tris(3-thioindolyl[1]methyl)benzene (TriSH$_3$). Protected precursor **4** (600 mg, 0.732 mmol) was suspended in a solution of $AgNO_3$ (1.24 g, 7.30 mmol) in MeOH (80 mL) and stirred vigorously for 1 h in the dark. During this time, a yellow precipitate formed, which was isolated by centrifugation and decantation of the colorless supernatant. The precipitate was then washed with MeOH (80 mL), after which aqueous 6 M HCl (40 mL) and ether (40 mL) were added. The resulting mixture was stirred vigorously in the dark for 1 h. The ether layer was removed, washed with water (3 × 60 mL) and brine (1 × 60 mL), dried over $MgSO_4$, and evaporated to yield a white solid. ^{1}H NMR revealed the presence of 0.14 equiv of diethyl ether. Yield: 427 mg (0.651 mmol, 89%). The ether was removed under ultrahigh-vacuum conditions prior to microanalysis and further ^{1}H and ^{13}C NMR characterization. This allowed for resolution of the product methyl ^{13}C signal, which had been overlooked by Pohl and coworkers.[23] Anal. Calcd for $C_{33}H_{33}N_3S_3$: C, 72.52; H, 6.09; N, 6.51; S, 14.89. Found: C, 72.41; H, 6.15; N, 6.37; S, 14.78. ^{1}H NMR (300 MHz, $CDCl_3$): δ 7.75 (d, $^3J_{H-H}$ = 7.6 Hz, 3 H, indolyl H), 7.48 (d, $^3J_{H-H}$ = 8.0 Hz, 3 H, indolyl H), 7.34 (td, $^3J_{H-H}$ = 7.6 Hz, $^4J_{H-H}$ = 1.2 Hz, 3 H, indolyl H), 7.26 (td, $^3J_{H-H}$ = 7.4 Hz, $^4J_{H-H}$ = 0.55 Hz, 3 H, indolyl H), 6.71 (d, $^4J_{H-H}$ = 1.4 Hz, 3 H, indolyl H2), 5.33 (s, 6 H, NCH_2), 2.90 (d, $^4J_{H-H}$ = 1.7 Hz, 3 H, SH), 2.61 (q, $^3J_{H-H}$ = 7.6 Hz, 6 H, CH_2CH_3), 0.95 (t, $^3J_{H-H}$ = 7.7 Hz, 9 H, CH_2CH_3). ^{13}C{^{1}H} NMR (75 MHz, $CDCl_3$): δ 146.33 (aryl C), 136.93 (indolyl C), 131.12, 130.83, 129.99 (2 × indolyl C, 1 × aryl C), 122.83, 120.76, 119.94, 109.45 (4 × indolyl C), 96.38 (indolyl CSH), 43.85 (NCH_2), 23.66 (CH_2CH_3), 15.47 (CH_2CH_3). FT-IR (ATR, ν, cm^{-1}): 3048, 2965, 2522, 1610, 1509, 1451, 1389, 1337, 1297, 1260, 1217, 1166, 1075, 1012, 928, 801, 737.

(n-Bu$_4$N)$_2$[Fe$_4$S$_4$(TriS)(SEt)] (5). (n-Bu$_4$N)$_2$[Fe$_4$S$_4$(SEt)$_4$][18] (450 mg, 0.415 mmol) was dissolved in DMF (15 mL). A solution of TriSH$_3$·0.14Et$_2$O (272 mg, 0.415 mmol) in THF (5 mL) was then added via cannula, and an immediate color change from brown to violet was observed. The solution was stirred alternatingly under static and dynamic vacuum for 1 h, yielding a black residue. CH_2Cl_2 (10 mL) was added, and the purple solution was filtered and concentrated to approximately 5 mL. The addition of diethyl ether (40 mL) resulted in the formation of a black precipitate, which was collected by centrifugation and dried under vacuum. ^{1}H NMR and elemental analysis revealed the presence of 0.25 equiv of DMF and 0.08 equiv of ether. Yield: 610 mg (0.390 mmol, 94%). Anal. Calcd for $C_{73}H_{113}Fe_4N_5S_8$·0.25C_3H_7NO·0.08$C_4H_{10}O$: C, 56.85; H, 7.44; N, 4.70; S, 16.39. Found: C, 56.76; H, 7.37; N, 4.62; S, 16.47. The ether was removed under ultrahigh-vacuum conditions prior to further ^{1}H and ^{13}C NMR characterization. ^{1}H NMR (300 MHz, CD_3CN): δ 13.14 (s, very broad, 2 H, SCH_2CH_3), 7.83 (d, broad, $^3J_{H-H}$ = 6.8 Hz, 3 H, indolyl H), 7.73 (d, $^3J_{H-H}$ = 8.2 Hz, 3 H, indolyl H), 7.31 (t, $^3J_{H-H}$ = 7.4 Hz, 3 H, indolyl H), 6.95 (t, broad, 3 H, indolyl H), 6.50 (s, broad, 6 H, NCH_2), 3.07 (t, broad, $^3J_{H-H}$ = 7.9 Hz, 16 H, n-Bu$_4$N$^+$ α-CH_2), 2.55–2.35 (m, broad, 9 H, SCH_2CH_3 and TriS CH_2CH_3), 1.61 (s, broad, 16 H, n-Bu$_4$N$^+$ β-CH_2), 1.36 (sextet, broad, $^3J_{H-H}$ = 6.5 Hz, 16 H, n-Bu$_4$N$^+$ γ-CH_2), 1.19 (s, broad, 9 H, TriS CH_2CH_3), 0.97 (t, $^3J_{H-H}$ = 6.9 Hz, 24 H, n-Bu$_4$N$^+$ CH_3). ^{13}C{^{1}H} NMR (75 MHz, CD_3CN): 146.21 (aryl C), 139.51 (indolyl C), 132.47 (aryl C), 122.26, 120.86, 120.82, 111.01 (4 × indolyl C), 60.32 (n-Bu$_4$N$^+$ α-C), 42.15 (TriS NCH_2), 24.80 (n-Bu$_4$N$^+$ β-C), 24.00 (TriS CH_2CH_3), 20.89 (n-Bu$_4$N$^+$ γ-C), 16.26 (TriS CH_2CH_3), 14.25 (n-Bu$_4$N$^+$ CH_3). The signals of the EtS$^-$ ligand and three of the indolyl C atoms were not observed. λ_{max} (MeCN, nm): 221 sh, 243 sh, 280 sh, 316 sh. FT-IR (ATR, ν, cm^{-1}): 2959, 2871, 1454, 1380, 1335, 1295, 1246, 1204, 1170, 1150, 1010, 880, 791, 735. $E_{1/2}$ vs Fc/Fc$^+$ in CH_2Cl_2 = −1.70 V (ΔE_p = 110 mV) [2−/3−], −0.56 (ΔE_p = 90 mV) [2−/1−]. $E_{1/2}$ vs SCE in CH_2Cl_2 = −1.27 V [2−/3−], −0.13 V [2−/1−]. ESI-MS: m/z 527.1 ([Fe$_4$S$_4$(TriS)(SEt)]$^{2-}$, calcd m/z = 527.9).

[Fe(tpySH)$_2$](PF$_6$)$_2$ (6). TpySH[11] (79.5 mg, 0.300 mmol) was stirred in EtOH (10 mL) for 15 min. A solution of $(NH_4)_2Fe(SO_4)_2$·$6H_2O$ (61.0 mg, 0.156 mmol) in H_2O (10 mL) was then added dropwise, and the mixture immediately turned purple. After stirring for an additional 10 min, the mixture was filtered over Celite into a solution of NH_4PF_6 (150 mg, 0.920 mmol) in H_2O (50 mL). A purple precipitate was collected by centrifugation, washed with water (10 mL) and ether (50 mL), and dried in vacuo. Yield: 108 mg (0.123 mmol, 82%). Anal. Calcd for $C_{30}H_{22}F_{12}FeN_6P_2S_2$: C, 41.11; H, 2.53; N, 9.59; S, 7.32. Found: C, 41.28; H, 2.60; N, 9.58; S, 7.15. ^{1}H NMR (400 MHz, CD_3CN): δ 8.82 (s, 4 H, H3′), 8.34 (d, $^3J_{H-H}$ = 6.4 Hz, 4 H, H3), 7.86 (t, $^3J_{H-H}$ = 7.0 Hz, 4 H, H4), 7.15 (d, $^3J_{H-H}$ = 5.2 Hz, 4 H, H6), 7.06 (t, $^3J_{H-H}$ = 6.4 Hz, 4 H, H5), 5.29 (s, broad, 2 H, SH). ^{13}C{^{1}H} NMR (100 MHz, CD_3CN): δ 160.01, 158.64, 154.30, 139.58, 128.22, 124.49, 123.96. The signal of one remaining carbon nucleus could not be resolved. λ_{max} [MeCN, nm (ϵ, M^{-1} cm^{-1})]: 242 (31 000), 282 (64 000), 317 (37 000), 359 sh (6800), 564 (15 000). FT-IR (ATR, ν, cm^{-1}): 3117, 2582, 1605, 1467, 1431, 1404, 1126, 907, 823, 788, 753. $E_{1/2}$ vs Fc/Fc$^+$ in MeCN = +0.74 V (ΔE_p = 38 mV) [2+/3+]. $E_{1/2}$ vs SCE in MeCN = +1.12 V [2+/3+]. ESI-MS: m/z = 293.46 ([Fe(tpySH)$_2$]$^{2+}$, calcd m/z = 293.54), 585.16 ([Fe(tpySH)(tpyS)]$^+$, calcd 585.06), 730.97 ({[Fe(tpySH)$_2$](PF$_6$)}$^+$, calcd 731.03).

[Fe(tpyS)$_2$] (7). TpySH[11] (63.6 mg, 0.240 mmol) was stirred in EtOH (8 mL) for 15 min. A solution of $(NH_4)_2Fe(SO_4)_2$·$6H_2O$ (48.7 mg, 0.124 mmol) in H_2O (8 mL) was then added dropwise, and the mixture immediately turned purple. After stirring for an additional 10 min, the mixture was filtered over Celite. The addition

(17) Vacca, A.; Nativi, C.; Cacciarini, M.; Pergoli, R.; Roelens, S. *J. Am. Chem. Soc.* **2004**, *126*, 16456–16465.
(18) Christou, G. C.; Garner, C. D. *J. Chem. Soc., Dalton Trans.* **1979**, 1093–1094.

Chart 1. The Tripodal $L(SH)_3$ and $TriSH_3$ Ligands

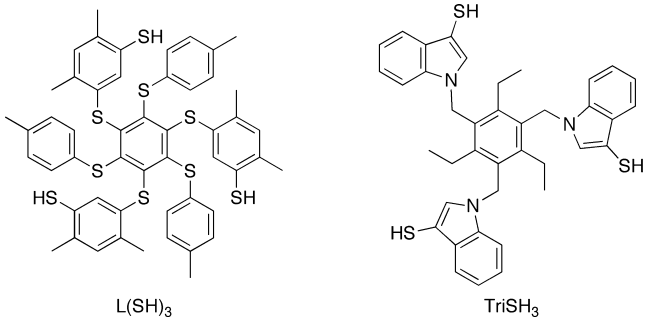

of aqueous 1 M NaOH (40 mL) resulted in the precipitation of a black powder, which was collected by centrifugation, washed with H_2O (2 × 40 mL), and dried in vacuo. Yield: 47.7 mg (0.0816 mmol, 68%). Anal. Calcd for $C_{30}H_{20}FeN_6S_2$: C, 61.65; H, 3.45; N, 14.38; S, 10.97. Found: C, 61.54; H, 3.58; N, 14.25; S, 10.90. ^{1}H NMR (400 MHz, CD_2Cl_2): 8.72 (s, 4 H, H3′), 8.07 (d, $^3J_{H-H}$ = 8.1 Hz, 4 H, H3), 7.65 (t, $^3J_{H-H}$ = 7.7 Hz, 4 H, H4), 7.28 (d, $^3J_{H-H}$ = 5.3 Hz, 4 H, H6), 6.93 (t, $^3J_{H-H}$ = 6.5 Hz, 4 H, H5). ^{13}C{^{1}H} NMR (100 MHz, CD_2Cl_2): δ 160.56, 155.51, 153.52, 137.52, 130.20, 126.11, 121.95. The signal of one remaining carbon nucleus could not be resolved. λ_{max} (MeCN, nm): 239, 277, 285, 316, 394, 603. Because of the instability of **7** in solution, extinction coefficients were not determined. FT-IR (ATR, ν, cm^{-1}): 1592, 1558, 1461, 1424, 1391, 1337, 1117, 1101, 1028, 1014, 836, 784, 754, 689. $E_{1/2}$ vs Fc/Fc$^+$ in CH_2Cl_2 = +0.63 V (ΔE_p = 78 mV) [2+/3+]. $E_{1/2}$ vs SCE in CH_2Cl_2 = +1.05 V [2+/3+].

(*n*-Bu$_4$N)$_2$[{Fe$_4$S$_4$(TriS)(μ-Stpy)}$_2$Fe] (8). A solution of **6** (20.0 mg, 0.0228 mmol) in DMF (2.5 mL) was added to a solution of **5**·0.26DMF·0.12Et$_2$O (71.6 mg, 0.0456 mmol) in DMF (2.5 mL). The mixture was stirred for 1 h and then treated alternatingly with static and dynamic vacuum for 30 min. Overnight vapor diffusion of ether led to the precipitation of a black, amorphous product, which was collected by centrifugation and dried in vacuo. Elemental analysis indicated the presence of 1 equiv of DMF. Yield: 42.3 mg (0.0135 mmol, 59%). Anal. Calcd for $C_{140}H_{164}Fe_9N_{14}S_{16}$·$C_3H_7NO$: C, 54.84; H, 5.50; N, 6.71; S, 16.38. Found: C, 54.45; H, 5.36; N, 6.35; S, 16.53. ^{1}H NMR (400 MHz, CD_3CN): 7.89–7.67 (m, broad, 20 H, 2 × indolyl H, tpyS H3, H4), 7.32–7.13 (m, broad, 20 H, indolyl H, tpyS H5, H6), 6.97 (s, broad, 6 H, indolyl H), 6.65 (s, 12 H, NCH_2), 3.06 (s, broad, 16 H, *n*-Bu$_4$N$^+$ α-CH_2), 2,43 (s, broad, 12 H, TriS CH_2CH$_3$), 1.59 (s, broad, 16 H, *n*-Bu$_4$N$^+$ β-CH_2), 1.34 (s, broad, 16 H, *n*-Bu$_4$N$^+$ γ-CH_2), 1.18 (s, broad, 18 H, TriS CH_2CH_3), 0.96 (t, $^3J_{H-H}$ = 6.6 Hz, 24 H, *n*-Bu$_4$N$^+$ CH_3). λ_{max} (MeCN, nm): 223 sh, 242 sh, 279, 285, 314, 375 (sh), 598. FT-IR (ATR, ν, cm^{-1}): 2958, 2870, 1663, 1588, 1451, 1386, 1333, 1295, 1199, 1150, 1100, 1010, 825, 786, 737. $E_{1/2}$ vs Fc/Fc$^+$ in CH_2Cl_2 = −1.48 V (ΔE_p = 82 mV) [2−/4−]. $E_{1/2}$ vs SCE in CH_2Cl_2 = −1.06 V [2−/4−].

Results and Discussion

Synthesis of a Suitable Site-Differentiated [4Fe−4S] Cluster System. To study the feasibility of tpySH as a bridging ligand in [4Fe−4S] metal assemblies, a suitable [4Fe−4S] cluster was sought. The use of tripodal trithiolate ligands that coordinate to three of the Fe atoms in a [4Fe−4S] cluster conveniently limits the reactivity to one specific Fe site. Holm and co-workers were the first to report such a 3:1 site-differentiated [4Fe−4S] cluster, thereby using the preorganized, tripodal $L(SH)_3$ ligand (Chart 1) to chelate three of the four cluster Fe atoms.[19] The synthesis of this ligand, however, is rather cumbersome and makes use of the highly toxic chemicals chloromethyl methyl ether, $Hg(OAc)_2$, and H_2S. Alternative ligands based on cyclic polyethers,[20] triazacyclanes,[21] and cyclotriveratrylene[22] are also somewhat tedious to synthesize and their 1:1 reaction stoichiometries with [4Fe−4S] clusters were never proven through X-ray crystallography. In contrast, a tripodal ligand that is relatively simple to prepare and has a crystallographically proven capacity for site differentiation is 1,3,5-triethyl-2,4,6-tris(3-sulfanylindolyl[1]methyl)benzene ($TriSH_3$, Chart 1). In 1997, Pohl and co-workers reported this promising alternative to $L(SH)_3$ to be accessible via a five-step synthesis route, although still employing the reagents mentioned above.[23] We devised a modified synthesis of $TriSH_3$ that not only obviates the use of these reagents but also significantly improves the overall yield (Scheme 2).

The improved synthesis begins with the two-step conversion of indole via 3-thiouroniumindole iodide (**1**) to indole-3-thiol (**2**) following literature methods[16] in an overall yield of 81%. In the subsequent thiol protection step, the use of carcinogenic chloromethyl methyl ether was circumvented by using chloromethyl ethyl ether instead, to yield 3-(ethoxymethylsulfanyl)indole (**3**). The large difference in acidity between the thiol and indole NH groups allowed for selective thiol deprotonation by triethylamine, thus obviating the use of NaH from the original procedure.[23] Three-fold nucleophilic addition of **3** to 1,3,5-tris(bromomethyl)-2,4,6-triethylbenzene[17] then yielded **4**, the ethoxymethyl-protected precursor of $TriSH_3$.

For deprotection of **4** to yield $TriSH_3$, we devised a deprotection protocol based on the hemithioacetal cleavage method developed by Topolski.[24] First, treatment of **4** with $AgNO_3$ in MeOH yielded a light-sensitive Ag adduct. Upon treatment with HCl, the adduct was converted to $TriSH_3$ in a yield of 89%.

The overall yield of $TriSH_3$ is 57% based on indole, which is more than double the yield of 24% reported in the original procedure.[23] The yield also substantially exceeds those reported for the other alternatives to $L(SH)_3$,[20−22] as well as that reported for $L(SH)_3$ itself.[25] In fact, the new synthesis probably makes $TriSH_3$ the most conveniently accessible site-differentiating [4Fe−4S] cluster ligand to date.

Reaction of $TriSH_3$ with (*n*-Bu$_4$N)$_2$[Fe$_4$S$_4$(SEt)$_4$] in DMF formed the 3:1 site-differentiated cluster compound (*n*-Bu$_4$N)$_2$[Fe$_4$S$_4$(TriS)(SEt)] (**5**) through thiol−thiolate ex-

(19) Stack, T. D. P.; Holm, R. H. *J. Am. Chem. Soc.* **1987**, *109*, 2546–2547.
(20) Whitener, M. A.; Peng, G.; Holm, R. H. *Inorg. Chem.* **1991**, *30*, 2411–2417.
(21) Evans, D. J.; Garcia, G.; Leigh, G. J.; Newton, M. S.; Santana, M. D. *J. Chem. Soc., Dalton Trans.* **1992**, 3229–3234.
(22) (a) van Strijdonck, G. P. F.; van Haare, J. A. E. H.; van der Linden, J. G. M.; Steggerda, J. J.; Nolte, R. J. M. *Inorg. Chem.* **1994**, *33*, 999–1000. (b) van Strijdonck, G. P. F.; van Haare, J. A. E. H.; Hönen, P. J. M.; van den Schoor, R. C. G. M.; Feiters, M. C.; van der Linden, J. G. M.; Steggerda, J. J.; Nolte, R. J. M. *J. Chem. Soc., Dalton Trans.* **1997**, 449–461.
(23) Walsdorff, C.; Saak, W.; Pohl, S. *J. Chem. Soc., Dalton Trans.* **1997**, 1857–1861.
(24) Topolski, M. *J. Org. Chem.* **1995**, *60*, 5588–5594.

Scheme 2. Improved Synthesis of $TriSH_3$ and Generation of the 3:1 Site-Differentiated Cluster **5**

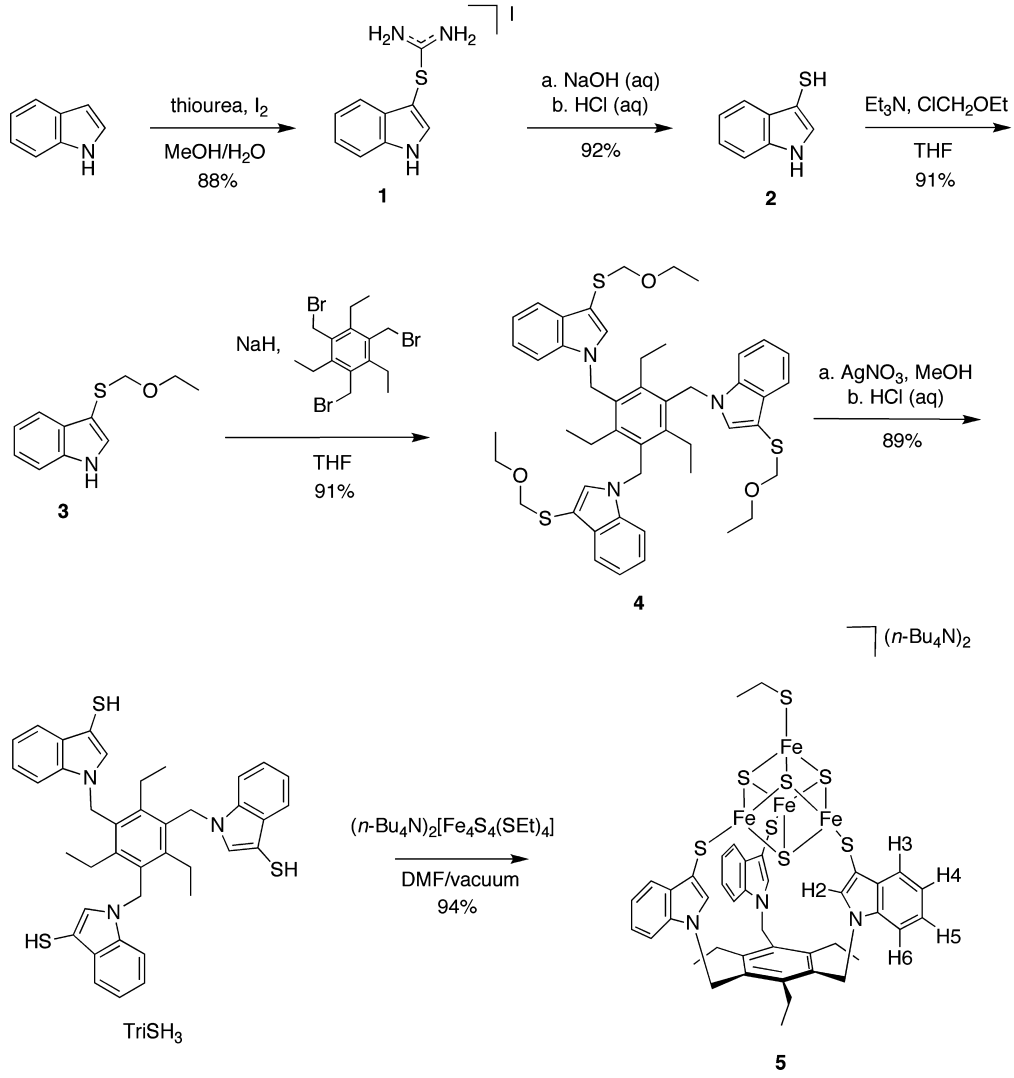

change[26] (Scheme 2). Full conversion was ensured by in vacuo removal of the volatile EtSH coproduct. Solid **5** was then isolated in over 90% yield by means of a simple precipitation step, with elemental analyses confirming the proposed formulation.

In the ^{1}H NMR spectrum of **5**, the TriS ligand gives rise to three signals corresponding to the NCH_2 and ethyl groups, as well as four aromatic signals for the H atoms on positions 4−7 of the indole rings (Figure 1). No signal is observed for the H2 protons, which are located close to the [4Fe−4S] cluster core and hence strongly experience the characteristic Fermi contact shifting expected for ligands bound to a [4Fe−4S] cluster.[27] The equivalence of the indolyl and ethyl groups indicates that **2** retains C_3 symmetry upon [4Fe−4S] coordination; hence, as in $(PPh_4)_2[Fe_4S_4(TriS)(SPh)]$,[23] rotation of the monodentate EtS^- ligand is fast on the NMR time scale.

In a CH_2Cl_2 solution, cluster **5** undergoes a chemically reversible 2−/3− transition, as well as a transition to an unstable 1− state (Figure 2). The 2−/3− transition occurs at −1.27 V vs SCE, and both i_{pc} and i_{pa} vary linearly with the square root of the scan rate. However, the peak separation

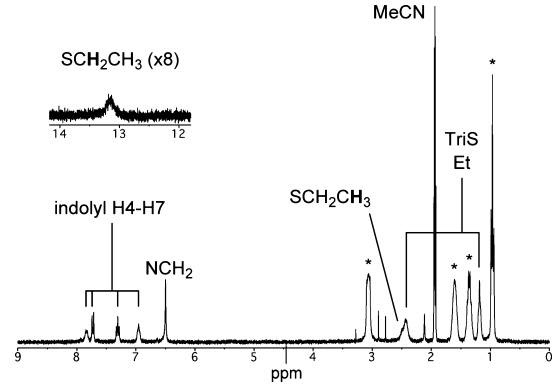

Figure 1. ^{1}H NMR spectrum of **5** in CD_3CN. n-Bu_4N^+ signals are marked with asterisks.

(25) (a) Stack, T. D. P.; Weigel, J. A.; Holm, R. H. *Inorg. Chem.* **1990**, *29*, 3745–3760. (b) Daley, C. J. A.; Holm, R. H. *J. Inorg. Biochem.* **2003**, *97*, 287–298.
(26) (a) Bobrik, M. A.; Que, L., Jr.; Holm, R. H. *J. Am. Chem. Soc.* **1974**, *96*, 285–287. (b) Que, L., Jr.; Bobrik, M. A.; Ibers, J. A.; Holm, R. H. *J. Am. Chem. Soc.* **1974**, *96*, 4168–4178.
(27) Holm, R. H.; Phillips, W. D.; Averill, B. A.; Mayerle, J. J.; Herskovitz, T. *J. Am. Chem. Soc.* **1974**, *96*, 2109–2117.

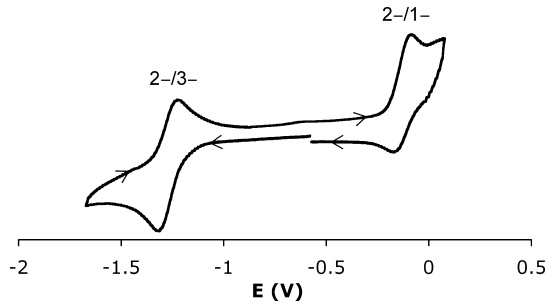

Figure 2. Cyclic voltammogram of **5** in CH_2Cl_2 (vs SCE).

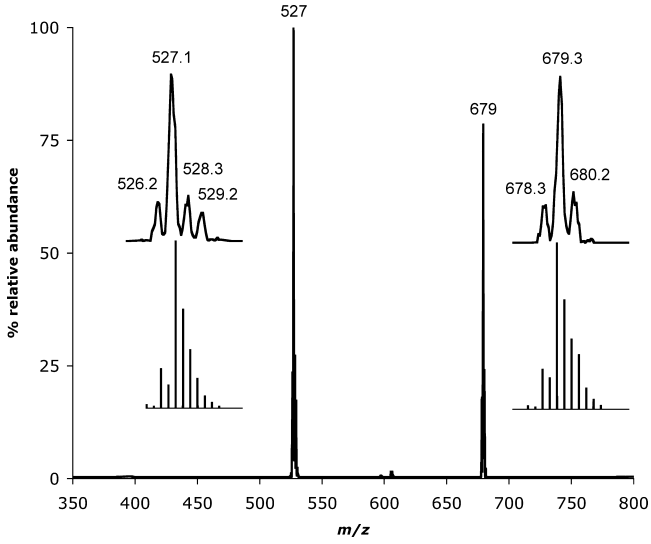

Figure 3. ESI mass spectrum of **5**.

is higher than expected for an electrochemically reversible process ($\Delta E_p = 100$ mV) and increases with the scan rate, implying quasi-reversibility.

Unlike the 2−/3− transition, the 2−/1− transition at $E_{1/2} = -0.13$ V is not fully reversible, displaying an oxidation wave that is significantly more intense than the corresponding reduction wave. Increasing the scan rate reduces the asymmetry between the waves, implying that the 1− state is unstable in solution and decomposes on the time scale of the electrochemical measurement. At more positive potentials, strictly irreversible oxidations occur.

Despite the scant precedent for mass spectrometry of synthetic [4Fe−4S] clusters, a satisfactory ESI mass spectrum could be obtained for **5** under inert conditions (Figure 3). The most intense signal in the spectrum, at $m/z = 527.1$, represents the $[\mathbf{5} - 2(n\text{-}Bu_4N)]^{2-}$ parent ion (calculated as $m/z = 527.9$). The isotope pattern shape for this signal agrees roughly with the calculation (Figure 3, inset), although on the utilized mass spectrometer, we were unable to achieve resolutions high enough to see isotope peak separations of 0.5 m/z units. The second most intense signal ($m/z = 679.3$) corresponds to an adduct of the $[\mathbf{5} - 2(n\text{-}Bu_4N)]^{2-}$ parent ion with n-Bu_4NSEt (calculated as $m/z = 679.1$). The mass spectrometry data for **5** constitute the second ESI mass spectrum analysis of a 3:1 site-differentiated [4Fe−4S] cluster, preceded only by the Fe-only hydrogenase H cluster mimic reported by Pickett and co-workers.[7] However, the generation of significant amounts of a species arising from the capture of free EtS^- is evidence for the lability of the cluster under electrospray conditions.

Synthesis of $[Fe(tpySH)_2](PF_6)_2$ (6). The cation $[Fe(tpySH)_2]^{2+}$ was chosen as a convenient moiety to link to the site-differentiated [4Fe−4S] cluster because it has a high degree of symmetry and avoids potential ligand scrambling as is often seen in heteroleptic tpy counterparts.[28] Possessing two thiol groups, $[Fe(tpySH)_2]^{2+}$ can potentially bind to two [4Fe−4S] clusters, thereby forming a metal-bridged [4Fe−4S] cluster dimer.

Inspired by the syntheses of other 4′-R-substituted $[Fe(tpy)_2]^{2+}$ species by Slattery and co-workers,[28,29] we prepared $[Fe(tpySH)_2](SO_4)$ in a single step from $(NH_4)_2Fe(SO_4)_2 \cdot 6H_2O$ and 2 equiv of tpySH. Treatment with NH_4PF_6 subsequently afforded the PF_6^- salt **6** in 82% yield (Scheme 3).

The ^{1}H NMR spectrum of **6** in CD_3CN shows a single set of tpySH signals, as would be expected for the D_{2d}-symmetric product (Figure 4). The chemical shift of the SH resonance is highly dependent on the water content of the sample, as well as traces of acid.

^{1}H NMR studies also showed that, in CD_3CN solutions exposed to air, the thiol groups in **6** are fully oxidized within a day. A small amount of precipitate forms while the thiol signal disappears and the aromatic region of the spectrum becomes similar to that of the cyclic, tpySStpy-bridged tetramer synthesized by Constable and co-workers.[11] Hence, the oxidation appears to yield a range of oligomeric products. This solution-phase air sensitivity has also been observed for tpySH as a free ligand.[11]

The UV–vis spectrum of **6** in MeCN (Figure 5) shows great similarity to the spectra of other substituted $[Fe(tpy)_2]^{2+}$ compounds. The lowest-energy electronic transition occurs at 564 nm, which correlates well with the 551 nm transition found in $[Fe(tpy)_2](PF_6)_2$.[30] Moreover, the 13 nm red shift of **6** as compared to that of the unthiolated analogue is in agreement with the results reported by Constable et al.[31] and Fallahpour et al.,[32] which indicate that substitution at the 4′ position always red shifts the lowest-energy transition of a $[Fe(tpy)_2]^{2+}$ chromophore, regardless of whether the substituent is electron-donating or -accepting. Further electronic transitions in **6** occur at 317, 282, and 242 nm.

In our subsequent investigation of the chemical properties of **6** in solution, we observed that deprotonation in the presence of an excess of Et_3N leads to a marked color change from purple to blue. Subsequent neutralization with aqueous HCl regenerates the purple color characteristic of **6**. In fact, the deprotonation product $[Fe(tpyS)_2]$ (**7**) could be prepared

(28) Hathcock, D. J.; Stone, K.; Madden, J.; Slattery, S. J. *Inorg. Chim. Acta* **1998**, *282*, 131–135.
(29) Chambers, J.; Eaves, B.; Parker, D.; Claxton, R.; Ray, P. S.; Slattery, S. J. *Inorg. Chim. Acta* **2006**, *359*, 2400–2406.
(30) Constable, E. C.; Housecroft, C. E.; Neuburger, M.; Phillips, D.; Raithby, P. R.; Schofield, E.; Sparr, E.; Tocher, D. A.; Zehnder, M.; Zimmermann, Y. *J. Chem. Soc., Dalton Trans.* **2000**, 2219–2228.
(31) Maestri, M.; Armaroli, N.; Balzani, V.; Constable, E. C.; Cargill Thompson, A. M. W. *Inorg. Chem.* **1995**, *34*, 2759–2767.
(32) Fallahpour, R.-A.; Neuburger, M.; Zehnder, M. *New J. Chem.* **1999**, 53–61.
(33) (a) Steer, R. P.; Ramamurthy, V. *Acc. Chem. Res.* **1988**, *21*, 380–386. (b) Maciejewski, A.; Steer, R. P. *Chem. Rev.* **1993**, *93*, 67–98.

Scheme 3. Syntheses of **6** and **7**

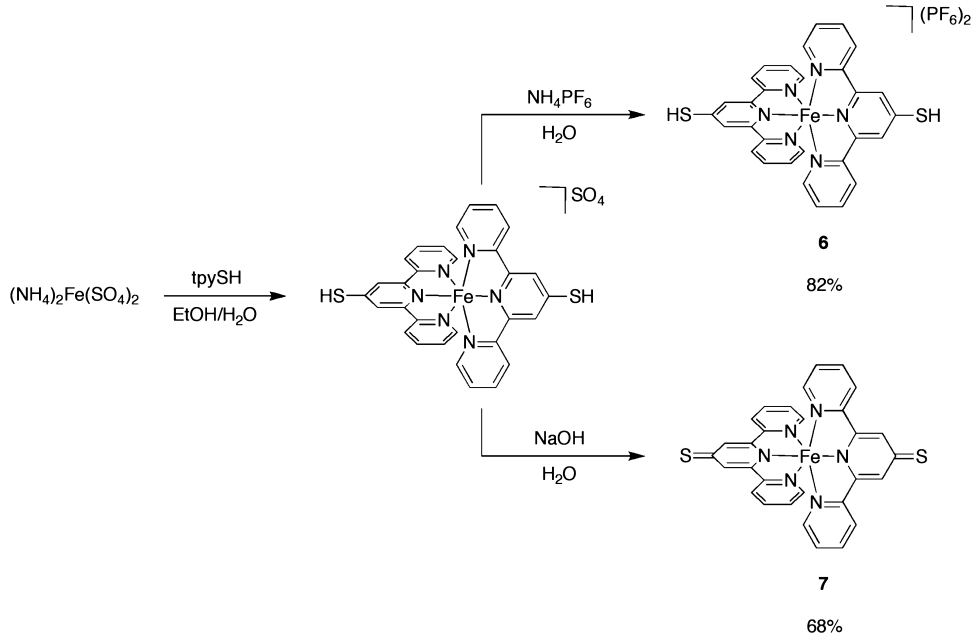

directly by reacting $(NH_4)_2Fe(SO_4)_2 \cdot 6H_2O$ with tpySH (2 equiv) in EtOH/H_2O, followed by the addition of aqueous NaOH (Scheme 3). Compound **7**, pure by elemental analyses, precipitated as a black powder.

The ^{1}H NMR spectrum of **7** in CD_2Cl_2 is similar to that of **6**, with the notable exception that a thiol signal is no longer observed (Figure 6). In contrast to **6**, compound **7** is highly unstable in solution; already within minutes from sample preparation under glovebox conditions, the ^{1}H NMR spectrum shows the presence of a secondary species. Within a day, **7** decomposes fully, a process accompanied by the formation of a purple precipitate.

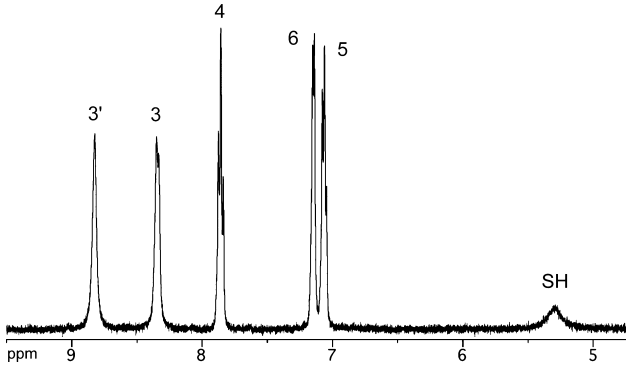

Figure 4. ^{1}H NMR spectrum of **6** in CD_3CN.

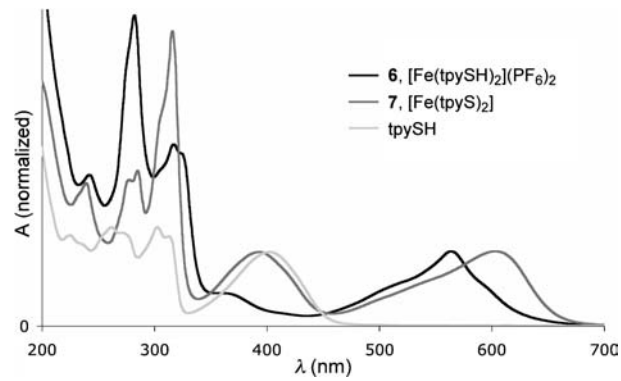

Figure 5. Normalized UV–vis spectra of **6**, **7**, and tpySH in MeCN.

UV–vis spectroscopy confirmed the electronic absorption differences between the acid–base couples **6** and **7** (Figure 5). The lowest-energy transition in **6** experiences a red shift of 39 nm upon deprotonation, and the absorption at 283 nm splits into two distinct peaks at 277 and 285 nm, thereby becoming significantly less intense than the absorption at 317 nm.

One of the most notable absorption changes, however, is the appearance of a new maximum of appreciable intensity at 394 nm. An analogous absorption is observed in the free tpySH ligand ($\lambda_{max} = 402$ nm; Figure 5) and corresponds to a $\pi-\pi^*$ transition concentrated on the thione C−S functionality.[33] Hence, as in the free ligand, the C−S bonds in **7** have significant double-bond character, implying thioquinonoid electron distributions, as shown in Scheme 3. Further evidence for this comes from IR spectroscopy, in which **7**, in contrast to **6**, shows a characteristic thione C−S stretch at 1101 cm^{-1}.

Electron distributions analogous to that in **7** have been observed in Ru and Co complexes with the oxy analogue of

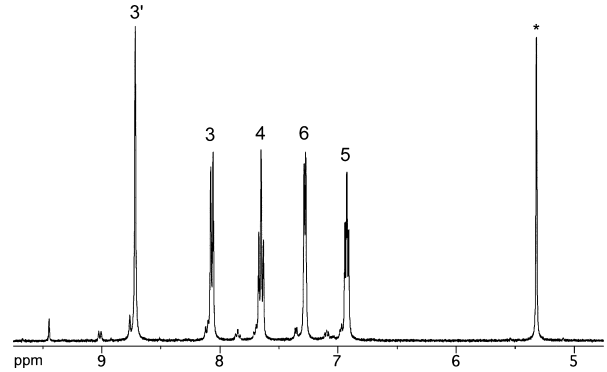

Figure 6. ^{1}H NMR spectrum of **7** in CD_2Cl_2. The asterisk denotes the residual solvent peak.

Scheme 4. Synthesis of **8**

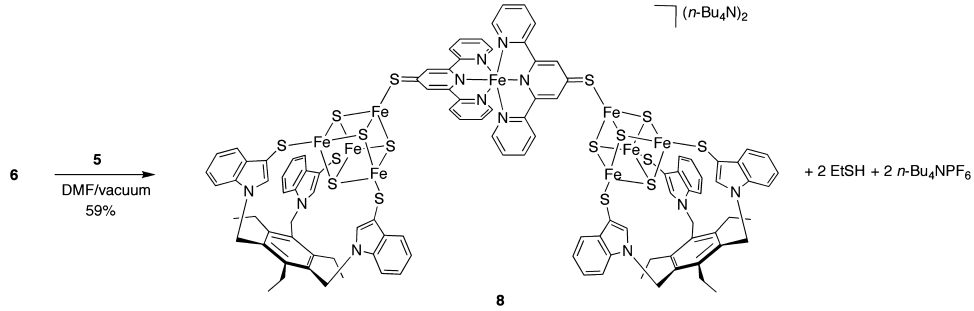

tpyS$^-$, tpyO$^-$,[34] as well as in compounds of pyridine-4-thiolate coordinated to Ru and Fe.[35] However, no mention of protonation-state-dependent electronic absorption changes has been made for these compounds. In fact, the only other examples that we could find of terpyridyl metal compounds with protonation-state-dependent UV–vis spectra are the compounds $[M(tpy\text{-}py)_2](PF_6)_2$ [M = Ru, Os; tpy-py = 4′-(4-pyridyl)-2,2′:6′,2″-terpyridine] reported recently by Maestri, Credi, and co-workers.[36] In these compounds, however, the ionizable atom is located farther away from the tpy moiety as compared to the directly attached thiol group in **6**, resulting in smaller spectral sensitivities to the protonation state.

In cyclic voltammetry, compound **6** shows a reversible 2+/3+ process in MeCN at +1.12 V vs SCE, although the peak separation of merely 38 mV suggests that the electrochemical process is complicated by adsorption effects. Slattery and co-workers observed a linear Hammett relationship between the 2+/3+ redox potential in 4′-R-substituted $[Fe(tpy)_2]^{2+}$ compounds in MeCN and the substituent σ_p value.[29] Given a σ_p value of +0.15 for the thiol group,[37] the observed potential of **6** is in excellent agreement with Slattery's empirical relation, thereby lying most closely to the potential of +1.13 V found for the nonsubstituted (R = H) analogue. Compound **7** was studied in CH_2Cl_2 because of its high solubility in this solvent and exhibited a reversible 2+/3+ process at +1.05 V vs SCE. The observed peak separation of 78 mV is consistent with a quasi-reversible, one-electron transition.

Synthesis of a [4Fe−4S] Cluster Dimer Bridged by 7. Following the successful synthesis of **6**, we reacted this dithiol with **5** (2 equiv) by means of thiol−thiolate exchange chemistry in a DMF solution, forming $(n\text{-}Bu_4N)_2[\{Fe_4S_4(TriS)(\mu\text{-}Stpy)\}_2Fe]$ (**8**; Scheme 4). This [4Fe−4S] cluster dimer could be separated from the n-Bu_4NPF_6 byproduct by means of a slow recrystallization, resulting in a yield of 59%.

The ^{1}H NMR spectrum of **8** in CD_3CN clearly shows the effects of bridge formation on both the cluster and $\{Fe(tpyS)_2\}$ moieties, despite the rather low signal-to-noise ratio resulting from the poor solubility of **8** in CD_3CN (Figure 7). The indolyl H4−H7 protons resonate at chemical shifts comparable to those in **5**, but the NCH_2 signal has shifted 0.15 ppm to a higher frequency. For the tpyS protons, substantial signal broadening is observed, as expected for ligands bound to a [4Fe−4S] cluster.[27] The most marked effect of the cluster binding, however, is the seeming absence of the 3′ signal. Similar to the likewise undetected indolyl H2 atoms (vide supra), the tpyS H3′ atoms in **8** are strongly contact-shifted because of their vicinity to the [4Fe−4S] cluster cores.

The UV–vis spectrum of **8** approximates a linear combination of the spectra of **5** and **7** (Figure 8), implying that the [4Fe−4S] and $\{Fe(tpyS)_2\}$ units in **8** act as rather independent chromophores. Compound **8** displays the $\pi-\pi^*$

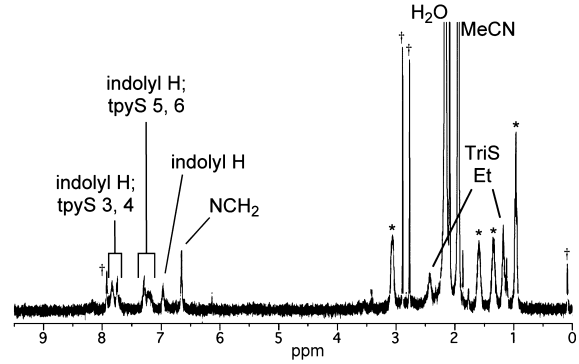

Figure 7. ^{1}H NMR spectrum of **8** in CD_3CN. n-Bu_4N^+ signals are marked with asterisks. DMF and silicone grease signals (marked with daggers) are probably strongly enhanced by the poor solubility of **8**.

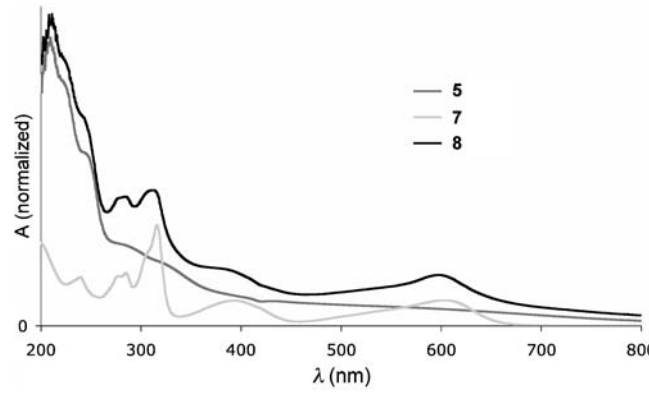

Figure 8. Normalized UV–vis spectra of **5**, **7**, and **8** in MeCN.

(34) (a) Constable, E. C.; Mundwiler, S. *Polyhedron* **1999**, *18*, 2433–2444. (b) Gaspar, A. B.; Muñoz, M. C.; Niel, V.; Real, J. A. *Inorg. Chem.* **2001**, *40*, 9–10.
(35) (a) Coe, B. J.; Hayat, S.; Beddoes, R. L.; Helliwell, M.; Jeffery, J. C.; Batten, S. R.; White, P. S. *J. Chem. Soc., Dalton Trans.* **1997**, 591–599. (b) Diógenes, I. C. N.; Sousa, J. R.; Carvalho, I. M. M.; Temperini, M. L. A.; Tanaka, A. A.; Moreira, I. S. *Dalton Trans.* **2003**, 2231–2236.
(36) Constable, E. C.; Housecroft, C. E.; Cargill Thompson, A.; Passaniti, P.; Silvi, S.; Maestri, M.; Credi, A. *Inorg. Chim. Acta* **2007**, *360*, 1102–1110.
(37) Hansch, C.; Leo, A.; Taft, R. W. *Chem. Rev.* **1991**, *91*, 165–195.

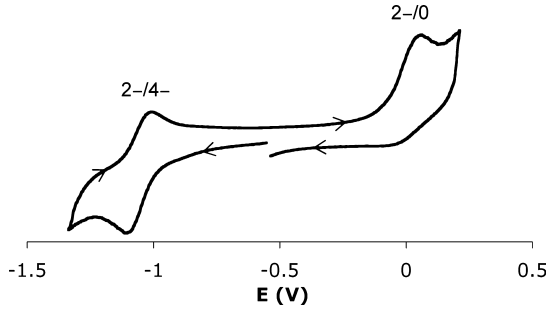

Figure 9. Cyclic voltammogram of **8** in CH_2Cl_2 (vs SCE).

transition concentrated on the C−S functionality as a shoulder at 375 nm, and the lowest-energy transition occurs at an energy similar to that in **7** (598 vs 603 nm, respectively). The parallels observed between **7** and **8** indicate that the effects of [4Fe−4S] cluster coordination on the energy levels of **7** are much smaller than the effects of protonation. Hence, the thione character of the $tpyS^-$ ligand appears to be dominant in **8**, as is also evidenced in IR spectroscopy by observation of the C−S stretching frequency at 1100 cm^{-1}.

The electrochemical profile of **8** in CH_2Cl_2 is similar to that of **5**, although shifted to significantly more positive potentials (Figure 9). A chemically reversible reduction now occurs at −1.06 V vs SCE and, like the 2−/3− process in **5**, displays linear relationships between the square root of the scan speed and the peak currents i_{pc} and i_{pa}. The observed peak separation is 82 mV at 100 mV/s, indicating that, although the overall charge of the assembly switches between 2− and 4−, the bridged [4Fe−4S] clusters essentially act as isolated redox units undergoing independent, one-electron transitions. Holm and co-workers have observed similar redox independence in a cluster dimer bridged by 1,4-benzenedithiolate and in clusters bridged by 1,3- and 1,4-benzenedimethanethiolate.[39] Analogous to the process at −1.06 V, we assign the irreversible oxidation at $E_{ox} = +0.05$ V to the parallel one-electron oxidations of the [4Fe−4S] cluster units in **8**, resulting in an overall neutral assembly.

The positive redox potential shift of 0.21 V observed in going from **5** to **8** is comparable to the potential differences reported by Holm and co-workers between $[Fe_4S_4(LS_3)(SEt)]^{2-}$ and $[Fe_4S_4(LS_3)(L')]^-$, with L′ a neutral pyridine or imidazole derivative.[38] The similarity reflects the fact that, as in $[Fe_4S_4(LS_3)(L')]^-$, each [4Fe−4S] cluster in **8** is essentially monoanionic; in other words, the formation of **8** can be seen as the substitution of EtS^- by the neutral ligand **7**.

Conclusion

The new [4Fe−4S] cluster **5** is the most easily accessible 3:1 site-differentiated cluster available thus far. Its facile, high-yielding synthesis and high purity, as confirmed by spectroscopic and elemental analyses, make it a most convenient starting material for more complex site-differentiated cluster systems such as **8**.

Bridged assembly **8** is the first [4Fe−4S] cluster dimer connected by a metal-containing linker. Holm and co-workers have previously reported [4Fe−4S] cluster dimers bridged by organic dithiols,[39] while the group of Pohl synthesized a dimer linked by a doubly chelating hexathiol.[40] Sulfide ions[20,39,41] and cysteine derivatives[42] have also been applied successfully as short-distance bridges in cluster dimer syntheses. Our approach employing tpySH as a directional bridging ligand has now enabled the use of a redox-active group as a linking moiety between the [4Fe−4S] clusters.

Fe-containing dithiol $[Fe(tpySH)_2](PF_6)_2$, **6**, is only the second reported coordination compound containing tpySH and represents an excellent building block in the synthesis of larger, bridged structures by virtue of its two available thiol functionalities. Furthermore, the drastic changes in electronic absorption exhibited by **6** upon deprotonation allow for the use of UV–vis spectroscopy to assess the extent of thioquinonoid electron distribution in compounds containing the $\{Fe(tpyS)_2\}$ chromophore.

Using tpySH, systematic studies of larger complexes containing both clusters and metal ions in different ratios should prove possible. Although the present study does not suggest high levels of interaction between the clusters themselves or between the clusters and the Fe^{2+} ion in **8**, the communication may be enhanced in future studies by variation of the bridging ligand or the single metal ion.

Acknowledgment. This work was financially supported by the National Research School Combination-Catalysis (NRSC-C). Dr. S. Grecea-Tanase, Dr. E. Bouwman, and Prof. J. Reedijk of the Leiden Institute of Chemistry are gratefully acknowledged for assistance with the cyclic voltammetry measurements, Dr. S. de Araujo Bambirra of the Stratingh Institute for conducting the ESI mass spectral measurement of **5**, and S. Wadman for stimulating discussions and collaboration on the synthesis of 4′-chloro-2,2′:6′,2″-terpyridine.

Supporting Information Available: Synthesis and characterization of compounds **1** and **2**. This material is available free of charge via the Internet at http://pubs.acs.org.

IC702062Q

(38) Zhou, C.; Holm, R. H. *Inorg. Chem.* **1997**, *36*, 4066–4077.
(39) Stack, T. D. P.; Carney, M. J.; Holm, R. H. *J. Am. Chem. Soc.* **1989**, *111*, 1670–1676.
(40) Walsdorff, C.; Saak, W.; Haase, D.; Pohl, S. *Chem. Commun.* **1997**, 1931–1932.
(41) (a) Huang, J.; Mukerjee, S.; Segal, B. M.; Akashi, H.; Zhou, J.; Holm, R. H. *J. Am. Chem. Soc.* **1997**, *119*, 8662–8674. (b) Challen, P. R.; Koo, S.-M.; Dunham, W. R.; Coucouvanis, D. *J. Am. Chem. Soc.* **1990**, *112*, 2455–2456. (c) Cai, L.; Weigel, J. A.; Holm, R. H. *J. Am. Chem. Soc.* **1993**, *115*, 9289–9290. (d) Cai, L.; Holm, R. H. *J. Am. Chem. Soc.* **1994**, *116*, 7177–7188. (e) Hoveyda, H. R.; Holm, R. H. *Inorg. Chem.* **1997**, *36*, 4571–4578.
(42) Barclay, J. E.; Diaz, M. I.; Evans, D. J.; Garcia, G.; Santana, M. D.; Torralba, M. C. *Inorg. Chim. Acta* **1997**, *258*, 211–219.